

Modeling, Simulating and Configuring Programmable Wireless Environments for Multi-User Multi-Objective Networking

Christos Liaskos*, Ageliki Tsioliariidou*, Shuai Nie[‡], Andreas Pitsillides[†], Sotiris Ioannidis*, and Ian Akyildiz^{†‡}

*Foundation for Research and Technology - Hellas (FORTH)

Emails: {cliaskos,atsiolia,sotiris}@ics.forth.gr

[†]University of Cyprus, Computer Science Department

Email: Andreas.Pitsillides@ucy.ac.cy

[‡]Georgia Institute of Technology, School of Electrical and Computer Engineering

Email: ian@ece.gatech.edu

Abstract—Programmable wireless environments enable the software-defined propagation of waves within them, yielding exceptional performance potential. Several building-block technologies have been implemented and evaluated at the physical layer. The present work contributes a network-layer scheme to configure such environments for multiple users and objectives, and for any physical-layer technology. Supported objectives include any combination of Quality of Service and power transfer optimization, eavesdropping and Doppler effect mitigation, in multi-cast or uni-cast settings. Additionally, a graph-based model of programmable environments is proposed, which incorporates core physical observations and efficiently separates physical and networking concerns. Evaluation takes place in a specially developed, free simulation tool, and in a variety of environments. Performance gains over regular propagation are highlighted, reaching important insights on the user capacity of programmable environments.

Index Terms—Wireless, Software control, Programmable, Smart Environments, Performance, Security, Mobility, Metasurfaces, HyperSurfaces.

I. INTRODUCTION

RECENT years have seen the rise of efforts to control the wireless propagation within a space, introducing programmable wireless environments (PWEs) [1]. According to the PWE paradigm, planar objects—such as walls in a floorplan—receive a special coating that can sense impinging waves and actively modify them by applying an electromagnetic (EM) *function*. Examples include altering the wave’s direction, power, polarization and phase [2]. The capabilities of several coating technologies have been demonstrated [3]–[5]. The present work builds upon these physical-layer works, and proposes a solution to the network-layer PWE configuration problem, i.e., which functions to deploy at the PWE coatings to serve a set of given user communication objectives.

Evaluated coating technologies for PWEs include relays, phased antenna arrays, and metasurfaces [6]. Each technology

comes with a range of supported functions, environmental applicability and efficiency degrees. Relays are 1 input- N output antenna pairs that can be placed over walls at regular intervals [5]. At each pair, one out of the N outputs can be selected, thereby redirecting the input wave in a partially customizable manner. Phased antenna arrays—also known as intelligent surfaces and reflectarrays [7]–[9]—are panels commonly comprising a number of patch antennas with half-wavelength size, in a 2D grid arrangement. At each patch, active elements such as PIN diodes are used for altering the phase of the reflected EM wave. Consistent wave steering and absorption is attained at the far field. Metasurfaces are similar structures, but with a 25 – 100⁺ times higher density of *meta-atoms* (i.e, the repeating unit of a planar antenna and active elements) [2]. This density allows them to form any surface current distribution over them, thereby producing any EM output due to the Huygens principle [10]. Thus, highly efficient EM functions even in the near field can be attained. HyperSurfaces are a novel class of networked metasurfaces that comes with a software programming interface (*API*) and an *EM compiler* [11], [12]. The API allows for getting the HyperSurface state and setting its EM function, while abstracting the underlying physics. The EM compiler translates the API callbacks to corresponding active element states.

A PWE is created by coating planar objects—such as walls and ceilings in an indoor environment—with *tiles*, i.e., rectangular panels of any aforementioned technology, with inter-networking capabilities [1]. The latter allow a central server to connect to any tile, get its state and set its EM function in an automated manner [13]. This maturity level reached at the physical layer of tiles opens a new research direction at the network level: *given a set of users with communication objectives within a PWE, what is the optimal EM function per tile to serve them?*

The present work contributes a solution to this problem, able to handle multiple users, objectives and EM functions. User mobility, multiple objectives per user, multicast groups and partially coated PWEs are supported. The objectives include power transfer and signal-to-interference maximization, as

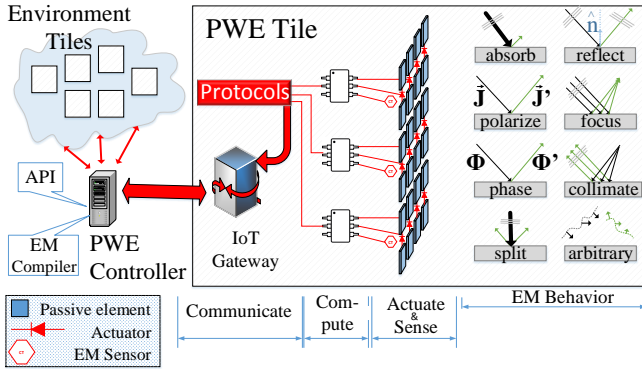


Fig. 1. Tile composition and PWE architecture.

well as eavesdropping and Doppler effect mitigation. In order to achieve these traits, the work also contributes:

- A systematic way of formulating and combining EM functions, which takes into account key-outcomes from the field of Physics (metamaterials).
- The *EM profile* of tiles, a novel concept that describes the supported EM functions per tile and their efficiency.
- A graph-based model to describe PWEs, and a way of transforming communication objectives to graph paths.
- A novel tool specifically developed for realistically simulating PWEs.

Extensive evaluations in multiple floorplans and topologies yield important conclusions about the maximum potential of PWEs and their user capacity in terms of maximal supported traffic load.

The remainder of this work is organized as follows. Section II surveys related studies. Section III describes the graph-based modeling of PWEs and the concepts of tile EM functions and profile. Section IV details the novel scheme for configuring PWEs. Evaluation takes place in Section V. The discussion follows in Section VI, along with future work directions, and the paper concludes in Section VII.

II. RELATED WORK

PWEs are attracting attention due to the recent advances in the development of new techniques to control the radiation patterns of EM waves [8], [13]–[16]. The existing literature mainly refers to PWE tile unit technologies, rather than PWE configuration approaches. We employ the layered taxonomy of Fig. 1 (introduced in [14]) to survey them:

EM behavior Layer. This layer comprises the supported EM function of the tile, and its principle of operation. Reflectarray tiles (and also phased arrays or intelligent surfaces) employ modifiable phase shifts applied over their surface. At the far field, reflected rays can be considered co-directional, and their superposition—constructive or destructive—is controlled by the applied phase shifts [7]. Thus, wave scattering or redirection functions can be attained. Metamaterial tiles operate at a lower level, acting as surfaces with tunable local impedance [2]. Impinging waves create inductive surface currents over the tile, which can be routed by tuning the local impedance across the tile. Notice that the principle of

Huygens states that any EM wavefront can be traced back to a current distribution over a surface [10]. Thus, in principle, metamaterials can produce any custom EM function as a response to an impinging wave. Common functions include wave steering, focusing, collimating (i.e., producing a planar wavefront as a response to an impinging wave), polarizing, phase altering, full or partial absorption, frequency selective filtering and even modulation [2], [17]. Metamaterials can be classified further as non-plasmonic or plasmonic. In the former, the impinging wave does not affect the configured local impedance. In plasmonic metamaterials, the surface impedance is altered by the impinging wave, producing non-linear effects [18], [19]. Thus, plasmonic metamaterials pose extra challenges in exerting deterministic control over waves, and are not considered for PWEs in the present work.

Actuation and Sensing Layer. This layer includes the actual hardware elements that can be controlled to achieve a phase shift or impedance distribution across a tile. Commonly, the layer comprises arrays of planar antennas—such as copper patches—and multi-state switches between them. Reflectarray tiles usually employ PIN diodes with controllable biasing voltage as switches [3]. Metamaterials have employed a wider range of choices, both in the shape and geometry of the planar antennas and in the nature of switches. CMOS transistors, PIN diodes, Micro-Electro-Mechanical Switches (MEMS), micro-fluidic switches, magnetic and thermal switches are but a few of the considered options in the literature [20]. Notably, some options—such as micro-fluid switches—are state-preserving in the sense that they require power only to change state but not to maintain it (i.e., contrary to biased PIN diodes).

Sensing impinging waves is also necessary for exerting efficient control over them. While this information can be provided by external systems [13], tiles can incorporate sensing capabilities as well [21]. The sensing can be direct, employing specialized sensors [22], or indirect, e.g., by deducing some impinging wave attributes from currents or voltages between tile elements [14].

Computing Layer. This layer comprises the computing hardware that controls the actuating and sensing elements. Its minimum duties include the mapping of local phase or impedance values to corresponding actuator states. Reflectarray tiles commonly implement this layer using FPGAs and shift registers [3]. Metasurfaces, and specifically HyperSurfaces, can alternatively employ standard Internet-of-Things (IoT) devices for the same purpose [15]. Moreover, they can optionally include application-specific integrated circuits (ASICs) distributed over the tile meta-atoms [23], [24]. This can enable autonomous, “thinking” tiles, where meta-atoms detect the presence and state of one another, and take local actuating decisions to meet a general functionality objective. Nonetheless, this advanced capabilities are not required for PWEs.

Communication Layer. This layer comprises the communication stack and the means that connect the actuating and sensing layers, the computing layer and tile-external devices (including other tiles and computers that monitor and configure PWEs [1]). In the simplest case, this layer is implemented within the computing hardware, acting as a gateway to the tile-

external world, using any common protocol (e.g., Ethernet). HyperSurface tiles with embedded ASICs additionally require inter-tile communication schemes, to handle the information exchange between smart meta-atoms. Both wired and wireless intra-tile communication is possible [23], [24]. In both cases, the ASIC hardware employs custom, non-standard protocols.

Differentiation. The related studies focus on one or more tile layers. However, to the best of the authors' knowledge, the topic of configuring a PWE per user directives has not been previously studied. In their previous work, the authors formally introduced the PWE concept, its architecture and challenges [1], [13]. Proof of concept PWE simulations took place in [6], [15], which treated the PWE configuration problem as a block box, employing a genetic algorithm to configure the PWE tile functions. Power maximization over an area served as the driving criterion for the genetic algorithm. The present work departs from genetic heuristics and offers an exact configuration process. The novel process can handle multiple users and objectives spanning security, quality of service (QoS), mobility and wireless power transfer. A graph-based model for PWEs is also introduced, that can facilitate future contributions in the network-layer of PWEs, using the related physical-layer studied in tile technologies as input.

III. A GRAPH-BASED MODEL FOR PROGRAMMABLE ENVIRONMENTS

This Section provides an abstract model of the Physics behind metasurfaces, leading to a function-centric formulation of their capabilities. This formulation is then used for modeling PWEs as a graph, and describing its workflow and performance objectives as path finding problems.

With no loss of generality, the text considers HyperSurface tiles, since they offer the richest set of supported features. The model, however, remains valid for any other tile technology. Moreover, the study will use an indoors setting as the driving scenario, but it remains valid in any other setting. Finally, the operating principles of PWEs and metasurfaces described in Sections I and II are sufficient for the remainder of the text. Additional introductory material can be found in the literature [1], [6], [13].

Persistent notation is summarized in Table I for ease. (Notation used only locally in the text is omitted).

A. General Modeling and Properties of of HyperSurface Functions

Let \mathcal{H} denote the set of all HyperSurface tiles deployed within an environment, such as the floorplan of Fig. 2. A single tile will be denoted as $h \in \mathcal{H}$. Let \mathcal{F}_h denote all possible EM functions that can be deployed to a tile h . A single function deployed to a tile will be $f_h \in \mathcal{F}_h$.

As discussed in Sections I and II, a function f_h is attained by setting the active elements of the HyperSurface accordingly. In this work we will assume that the correspondence between functions and active element states is known, and the reader is redirected to studies on *EM Compilers* for further details [11], [12].

TABLE I
SUMMARY OF NOTATION

Symbol	Explanation
\mathcal{H}	The set of all tiles within an environment.
$h \in \mathcal{H}$	A single HyperSurface tile.
\mathcal{F}_h	The set of EM functions supported by a tile h .
$f_h \in \mathcal{F}_h$	A single function, deployed to tile h .
$f_h^{\text{ABS}}, f_h^{\text{STR}}, f_h^{\text{COL}}$	Absorption, Steering and Collimation functions.
$m_h^{\text{PHA}}, m_h^{\text{POL}}$	EM phase and polarization function modifiers.
$\vec{E}_{in}, \vec{E}_{out}$	Nominal input/output (EM field) of a function.
$\mathbb{I}, \mathbb{O} :$ $\langle \omega, \vec{D}, \vec{P}, \vec{J}, \Phi \rangle$	EM function input/outputs as wave attributes: <frequency, direction, power, polarity, phase>.
PW, FW	Subscripts denoting plain wave and focal wave.
g_h	Wave power gain/loss after impinging at tile h .
$\mathcal{G}(\{\mathcal{H}, \mathcal{U}\}, \{\mathcal{L}_h, \mathcal{L}_u\})$	Graph with tiles \mathcal{H} and users $u \in \mathcal{U}$ as nodes, inter tile links \mathcal{L}_h and user-to-tile links \mathcal{L}_u .
$\vec{p}_{n n'}$	A path in \mathcal{G} as list of links from node n to n' .
$l_{n n'}$	A link in \mathcal{G} from node n to n' .
$\text{TX}(l_{uh}), \text{RX}(l_{hu})$	Link labels denoting intended Tx and Rx users.
$\langle \dots \rangle$	A tuple (group) of items.
$\{ \dots \}$	A list of objects (single items or tuples).
*	Unintended (not nominal) type of quantity *.
$\ * \ $	The cardinality of a set *.

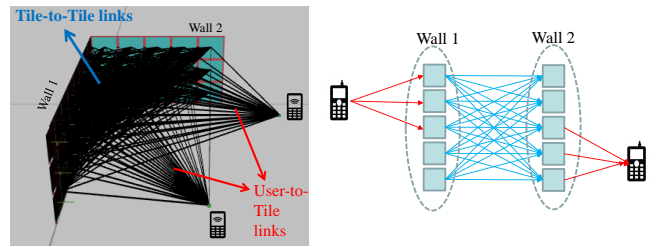


Fig. 2. 3D and 2D illustration of the types of links (user links and inter-tile links) and nodes (tiles and users) in a PWE.

Each function f_h receives a nominal input EM field, \vec{E}_{in} , (i.e., impinging upon the tile), and then returns a well-defined output \vec{E}_{out} (i.e., a reflected, refracted or no field-in case of perfect absorption), which can be abstracted as:

$$\vec{E}_{out} \leftarrow f_h(\vec{E}_{in}) \quad (1)$$

Consider the coordinate system over a tile, as shown in Fig. 3. In the most generic function case, \vec{E}_{in} is defined over the $\phi = 90^\circ$ plane on the surface, while \vec{E}_{out} contains the output field at any point $\{r, \theta, \phi\}$ around the tile. It is noted that a function f_h also defines the output to any, even *unintended* input, \widetilde{E}_{in} , which can exemplarily arise when EM sources move, without adapting the tile functions accordingly. Therefore, relation (1) is generalized as:

$$\widetilde{E}_{out} \leftarrow f_h(\widetilde{E}_{in}) \quad (2)$$

We proceed to remark two important properties of the EM functions, stemming from physics:

Remark 1. EM functions f_h are symmetric [2], [18]:

$$\widetilde{E}_{out} \leftarrow f_h(\widetilde{E}_{in}) \Leftrightarrow \widetilde{E}_{in} \leftarrow f_h(\widetilde{E}_{out}) \quad (3)$$

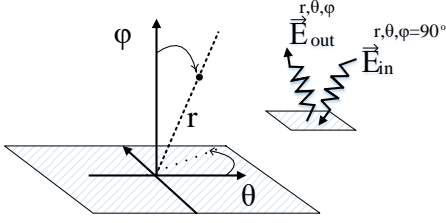


Fig. 3. The tile coordinate system for describing its inputs and outputs. The origin is at the tile center.

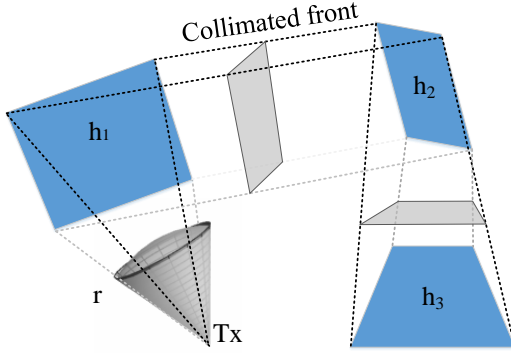


Fig. 4. Illustration of the propagation wavefront between users and tiles.

The symmetry remark can be used for defining a common format for inputs and outputs in Section III-B. It will also be called upon later on, to ensure that communication channels created by tuning HyperSurfaces are bidirectional.

Remark 2. EM functions f_h are a linear map of $\widetilde{E}_{in} \rightarrow \widetilde{E}_{out}$ [2]:

$$f_h \left(c \cdot \vec{E}_{in} + \sum_{\forall k} c_k \cdot \widetilde{E}_{in}^k \right) = c \cdot f_h \left(\vec{E}_{in} \right) + \sum_{\forall k} c_k \cdot f_h \left(\widetilde{E}_{in}^k \right) \quad (4)$$

where k is any index, and $c, c_k \in \mathcal{R}$.

The linearity property, in conjunction with the symmetry property will be promptly employed to reform the input/output format of f_h , without loss of generality.

B. Specialized Modeling of Function Inputs/Outputs

In communication scenarios, considering function input/outputs at the level of EM field may not be practical. Instead, considering the signal source location and characteristics that yields the \widetilde{E}_{in} can be more useful. To this end, we define the following input formats:

Planar wave. This case corresponds to a wave with a planar or almost planar wavefront, as shown in Fig. 4.

Planar waves can approximate:

- waves impinging on a tile from a distant antenna at its far region,
- waves that have been collimated at a preceding tile (e.g., h_1 in Fig. 4), by applying the corresponding EM function.

Focusing on the second case, we will treat the collimation output as the source of the planar wave. Employing the coordinate system of the tile receiving this wave (h_2 in Fig. 4) and due to the planarity assumption, a single-frequency (ω) wave of this class can be simply described by:

- its direction, $\overline{D} : \{r = \emptyset, \theta, \phi\}$ (using the \emptyset notation to denote irrelevance from the r -dimension).
- the total carried power, \mathbf{P} , that impinges upon the surface of the tile (the summation of the Poynting vector norm over any bounded wavefront),
- the normalized Jones vector, $\vec{\mathbf{J}}$ [25], describing the wave polarization at tile h_2 .
- the wavefront phase Φ at tile h_2 .

Since the field \widetilde{E}_{in} can be reconstructed from the aforementioned quantities, we proceed to replace it with the input parameter set for plane waves, \mathbb{I}_{PW} :

$$\widetilde{E}_{in} \mapsto \mathbb{I}_{PW} : \langle \omega, \overline{D}, \mathbf{P}, \vec{\mathbf{J}}, \Phi \rangle \quad (5)$$

Likewise, a planar output field \widetilde{E}_{out} defined over the surface of h_2 can be alternatively expressed by the output parameter set for plane waves, \mathbb{O}_{PW} :

$$\widetilde{E}_{out} \mapsto \mathbb{O}_{PW} : \langle \omega', \overline{D}', \mathbf{P}', \vec{\mathbf{J}}', \Phi' \rangle \quad (6)$$

where the ($'$) notation implies generally different values than relation (5).

Focal wave. This case represents any generally non-collimated radiation from a mobile device (cf. TX in Fig. 4), with its energy dissipating over an ever-growing sphere. In this case, the EM field impinging upon a tile also depends on the characteristics of the antenna device (radiation pattern and orientation). Assuming that this information is known and constant, and using a similar approach as above an input field at a tile, generated by such a source can be replaced as:

$$\widetilde{E}_{in} \mapsto \mathbb{I}_{FW} : \langle \omega, \overline{D}, \mathbf{P}, \vec{\mathbf{J}}, \Phi \rangle \quad (7)$$

where $\overline{D} : \{r, \theta, \phi\}$, and $\vec{\mathbf{J}}, \Phi$ potentially vary over the tile surface. (I.e., $\vec{\mathbf{J}}(r, \theta), \Phi(r, \theta)$). In the case where the focal wave is created (output) by a tile with the application of a proper function, the output field is similarly expressed as:

$$\widetilde{E}_{out} \mapsto \mathbb{O}_{FW} : \langle \omega', \overline{D}', \mathbf{P}', \vec{\mathbf{J}}', \Phi' \rangle \quad (8)$$

Remark 3. The notations (5), (6), (7) and (8) are compatible with the Symmetry property (Remark 1), since \mathbb{O}_{PW} and \mathbb{O}_{FW} are also valid as inputs of any function f_h , while \mathbb{I}_{PW} and \mathbb{I}_{FW} are also valid as outputs of any function f_h at tile h .

Finally, the linear map property of Remark 2, relation (4) is rewritten as:

$$f_h (\{\mathbb{I}_1, \mathbb{I}_2, \mathbb{I}_3, \dots\}) = \{f_h(\mathbb{I}_1), f_h(\mathbb{I}_2), f_h(\mathbb{I}_3), \dots\} \quad (9)$$

meaning that when multiple inputs are passed to a tile function, the total output is produced by applying the function to each input separately.

C. Modeling Core HyperSurface Functions

We proceed to study specialized HyperSurface functions, which are of practical value to the studied programmable wireless environments. Pure functions that can act as building blocks will be studied first, followed by a model for combining them into more complex ones.

Absorb f_h^{ABS} . Plane wave absorption has constituted one of the most prominent showcases of metasurfaces [2]. In the studied programmable environments, absorbing unwanted reflections is important for interference minimization, as well as enforcing determinism over EM propagation. The ideal absorption function for an intended plane wave input is expressed as:

$$f_h^{\text{ABS}}(\mathbb{I}_{PW}) \rightarrow \emptyset \quad (10)$$

where the empty set denotes no output wave. Full absorption is attained by matching the surface impedance of the tile to the incoming wave. For a planar input, this means that the surface impedance is constant across the tile, resulting into zero phase gradient and normal (specular) reflective behavior. This remark facilitates the modeling of unintended inputs as follows:

$$f_h^{\text{ABS}}\left(\widetilde{\mathbb{I}_{PW}} : \langle \omega, \overline{D}, \mathbf{P}, \vec{\mathbf{J}}, \Phi \rangle, \mathbb{I}_{PW}\right) \rightarrow \langle \omega, \text{SPEC}(\overline{D}), g \cdot \mathbf{P}, \vec{\mathbf{J}}, \Phi \rangle \quad (11)$$

where $g(\mathbb{I}_{PW}, \widetilde{\mathbb{I}_{PW}}) \in \mathcal{R} < 1$ is a metric of similarity between \mathbb{I}_{PW} and $\widetilde{\mathbb{I}_{PW}}$, defined by the physical structure of the HyperSurface and incorporating any constant material losses. The specular reflection of \overline{D} is calculated as:

$$\text{SPEC}(\overline{D}) = \overline{D} - 2(\overline{D} \cdot \vec{n})\vec{n} \quad (12)$$

where \overline{D} is directed and \vec{n} is the unit normal of the tile surface.

It is noted that relation (11) can be employed to achieve an intended: i) partial attenuation of a wave, and ii) frequency selective absorption (filtering) [2].

Steer f_h^{STR} . Steering plain waves from an incoming direction to another is achieved by enforcing a gradient surface impedance that corresponds to the required reflection index [2]. This physical phenomenon can be described by considering a virtual surface normal, \vec{n}' , supplied as an input parameter of steering, that corresponds to a required reflection direction via relation (12). We proceed to define f_h^{STR} as follows:

$$f_h^{\text{STR}}\left(\widetilde{\mathbb{I}_{PW}} : \langle \omega, \overline{D}, \mathbf{P}, \vec{\mathbf{J}}, \Phi \rangle, \vec{n}', \mathbb{I}_{PW}\right) \rightarrow \langle \omega, \overline{D} - 2(\overline{D} \cdot \vec{n}')\vec{n}', g \cdot \mathbf{P}, \vec{\mathbf{J}}, \Phi \rangle \quad (13)$$

where $g(\mathbb{I}_{PW}, \widetilde{\mathbb{I}_{PW}}) \in \mathcal{R} < 1$ in defined as in relation (11), noting that its specific expression generally differs from that of relation (11). We remark that the variant surface normal approach allows for a uniform expression (13), covering both the intended and unintended inputs.

Collimate f_h^{COL} . As noted in Section II, collimation is the action of transforming a non-planar input wave to a planar output [2]. In essence, the HyperSurface is configured for a virtual surface normal that varies across the tile surface,

matching the local direction of arrival of the input. In the present scope, collimation will be studied for focal wave input as follows:

$$f_h^{\text{COL}}\left(\mathbb{I}_{FW}, \overline{D}'\right) \rightarrow \mathbb{O}_{PW} : \langle \omega, \overline{D}', g \cdot \mathbf{P}, \vec{\mathbf{J}}, \Phi \rangle \quad (14)$$

where the focal wave characteristics and the intended reflection direction are provided as inputs. Relation (14) refers to intended inputs and outputs. Obtaining the output to an unintended input can be based on the surface normal across the tile. Each sub-area over which the surface normal can be considered constant interacts with a part of the wavefront that can be considered planar, resulting into a reflection calculated via relation (12). Thus, the outcome to unintended input is a set of planar outputs, each with its own power, polarity and phase:

$$f_h^{\text{COL}}\left(\widetilde{\mathbb{I}_{FW}}, \mathbb{I}_{FW}, \overline{D}'\right) \rightarrow \{\mathbb{O}_{PW}\} \quad (15)$$

In the context of the studied programmable environments, collimation is intended to be used mainly at the first and last hop of the propagation from one device to another [6]. The first application (at a tile) transforms the waves emitted from a device to a planar form (see Fig. 4). Tile-to-tile propagation is then performed for planar inputs. At the final tile before reaching the receiver, the planar wave is focused to the intended spot. This focusing is essentially collimation in the reverse, where a planar wave is converted to focal output. The tile configuration for focusing remains the same as in collimation, due to the symmetry in Remark 1.

Polarize m_h^{POL} . The physics of polarization control can be described qualitatively by assuming equivalent circuits of meta-atoms [2]. In essence, each meta-atom can be viewed as a circuit with an input and output antennas, as well as cross-couplings among meta-atoms. A wave enters via the input antennas, undergoes some alteration via the circuit and exits via output antennas, subject to the connections performed by tuning the active elements. Polarization is thus a shift in the Jones vector, attained by the appropriate choice of output antennas. Pure polarization control does not affect other wave parameters. As such, we define the polarization control not as a stand-alone function, but rather as a modifier applied to the output of a preceding function:

$$m_h^{\text{POL}}\left(\mathbb{O}_{PW} : \langle \omega, \overline{D}, \mathbf{P}, \vec{\mathbf{J}}, \Phi \rangle, \Delta \vec{\mathbf{J}}\right) \rightarrow \mathbb{O}'_{PW} : \langle \omega, \overline{D}, \mathbf{P}, \vec{\mathbf{J}} + \Delta \vec{\mathbf{J}}, \Phi \rangle \quad (16)$$

For unintended outputs, the intended shift $\Delta \vec{\mathbf{J}}$ is not necessarily attained, which can be expressed as:

$$m_h^{\text{POL}}\left(\widetilde{\mathbb{O}_{PW}}, \mathbb{O}_{PW}, \Delta \vec{\mathbf{J}}\right) \rightarrow \widetilde{\mathbb{O}'_{PW}} : \langle \omega, \overline{D}, \mathbf{P}, \vec{\mathbf{J}} + \Delta \vec{\mathbf{J}}', \Phi \rangle \quad (17)$$

where $\Delta \vec{\mathbf{J}}' \neq \Delta \vec{\mathbf{J}}$ in general. Notice that power loss concerns are delegated to the preceding pure function.

Phase Alteration m_h^{PHA} . Phase alteration follows the same principle as the polarization. Qualitatively, the modification of the wave phase is accomplished within the equivalent circuit,

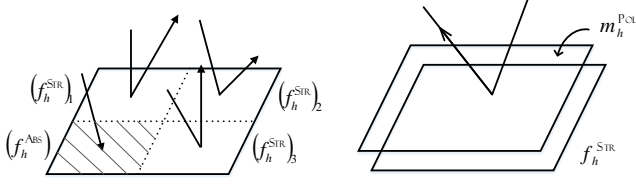


Fig. 5. Function combination models: Surface Division (left) and Meta-atom Merge (right).

via an inductive or capacitive element [2]. Once again, this functionality is defined as a modifier:

$$m_h^{\text{PHA}} \left(\mathbb{O}_{PW} : \langle \omega, \bar{D}, \mathbf{P}, \vec{\mathbf{J}}, \Phi \rangle, \Delta\Phi \right) \rightarrow \mathbb{O}'_{PW} : \langle \omega, \bar{D}, \mathbf{P}, \vec{\mathbf{J}}, \Phi + \Delta\Phi \rangle \quad (18)$$

For unintended outputs, the definition is altered similarly to relation (17).

Combination model: The pure functions studied above can be combined to describe a more complex functionality. Complex functions may be an operational requirement (e.g., steer and polarize at the same time), or be imposed by physical imperfections of the metasurface (e.g., being unable to steer without altering the polarization). We proceed to present a common model to describe both cases.

Surface division. This combination approach assigns different functions to different sub-areas of the same tile [17]. The principle of operation is shown in Fig. 5 (left inset), where an impinging plane undergoes splitting into 3 separate directions and partial attenuation. The power distribution of any output waves depends on the area allocated to each sub-function. For instance, an ideal N -way split of an input \mathbb{I}_{PW} towards directions with custom normals $\vec{n}'_i, i = 1 \dots N$ can be expressed as:

$$f_h^{\text{SPL}} (\mathbb{I}_{PW}, \{\vec{n}'_i\}) \rightarrow \{\mathbb{O}_{PW}\}, \{\mathbb{O}_{PW}\} : \left\{ \langle \omega, \bar{D} - 2(\bar{D} \cdot \vec{n}'_i) \vec{n}'_i, \frac{1}{N} \cdot \mathbf{P}, \vec{\mathbf{J}}, \Phi \rangle \mid i = 1 \dots N \right\} \quad (19)$$

where (P/N) is the power of each output.

Meta-atom merge. A common practice in metasurface analysis is to merge meta-atoms to create more complex basic structures, called supercells [26]. Essentially, using the equivalent circuit paradigm, merging meta-atom creates circuits with more degrees of tunability. This enables the combination of functions and modifiers, e.g., for steering and polarizing or steering and phase altering at the same time, over the same surface (cf. Fig. 5, right inset), denoted as:

$$m_h^{\text{POL}} (f_h^{\text{STR}}), m_h^{\text{PHA}} (f_h^{\text{STR}}), \text{ or } m_h^{\text{POL}} (m_h^{\text{PHA}} (f_h^{\text{STR}})) \quad (20)$$

Additionally, it is possible to apply a meta-atom merge-derived function only to a sub-area of a tile, thus combining it with surface division.

A summary of combinable functions and combination approaches is given in Table II. Notably: i) the combination patterns are symmetric, ii) combining collimation with any other non-modifier function is possible but potential unintended, as

TABLE II
COMBINABLE TILE FUNCTIONS AND METHODS.

		MERGE WITH				
		f_h^{ABS}	f_h^{STR}	f_h^{COL}	m_h^{POL}	m_h^{PHA}
FUNCTION	f_h^{ABS}	SD	SD	$\underline{\text{SD}}$	MM*	MM*
	f_h^{STR}	SD	SD	$\underline{\text{SD}}$	MM	MM
	f_h^{COL}	$\underline{\text{SD}}$	$\underline{\text{SD}}$	$\underline{\text{SD}}$	MM	MM
	m_h^{POL}	MM*	MM	MM	-	MM
	m_h^{PHA}	MM*	MM	MM	MM	-

SD: Surface Division, **MM:** Meta-atom Merge,

\sim : Possible but potentially unintended.

*: Defined only when f_h^{ABS} produces output (partial absorb).

described in the context of relation (15), iii) combining a modifier with absorption makes sense only when the absorption is partial (i.e., there is an output to apply the modifier upon), and iv) combining several modifiers of the same type to the same tile is the same as applying it once with the total modification. As such, these combinations are trivial. *Finally, it is noted that any number of functions (i.e., more than two) can be merged via the surface division model.*

It is worth noting that merging functions is not without impact on the efficiency of the HyperSurface. Any metasurface requires a minimum amount of meta-atoms to yield a consistent behavior (i.e., with near-unitary efficiency) [17]. Both surface division and meta-atom merge naturally limit the meta-atom numbers available for a given functionality. As such, combining functions will generally amplify discretization, boundary and other errors [7]. This can lead to reduced efficiency, which can be expressed as considerably attenuated intended outputs, as well as the appearance of unintended, parasitic outputs, $\mathbb{O}_{\mathbb{P}}$, even for intended inputs:

$$f_h (\mathbb{I}, \tilde{\mathbb{I}}) \rightarrow f_h (\mathbb{I}) + f_h (\tilde{\mathbb{I}}) + \mathbb{O}_{\mathbb{P}} \quad (21)$$

where $f_h (\mathbb{I})$ is the intended output and $f_h (\tilde{\mathbb{I}})$ is the well-defined output to unintended input. Thus:

Remark 4. Combining functionalities over a single tile generally reduces the efficiency of the overall function.

The effects of Remark 4 can be quantified only per specific, physical HyperSurface design. Nonetheless, we will employ this remark in ensuing Sections and setup a policy of minimizing function combinations in programmable wireless environments.

Remark 5. The generic relation (21), in conjunction with the preceding modeling defines the information that a HyperSurface manufacturer should measure and provide, to facilitate the use in programmable environments. This information, collectively referred to as *EM profile* contains the following information:

- The supported function types and allowed combinations, as a subset of the entries of Table II.
- The intended and parasitic outputs to intended inputs.

- The unintended and parasitic outputs to unintended inputs.

The EM profile can be obtained, e.g., by measuring the scattering pattern in controlled conditions, for the complete array of supported functions and intended inputs. Nonetheless, an exhaustive measurement for any unintended input may be prohibitive. In this case, the profile may provide a calculation model for outputs, such as the $g(\mathbb{I}_{PW}, \widetilde{\mathbb{I}}_{PW})$ metric employed in Section III-C.

For the remainder of this study, we will consider the EM profile as a given, provided by the tile manufacturer.

D. A Graph Model for Simulating and Optimizing Programmable Wireless Environments

Propagation within a 3D space comprises Line-of-sight (LOS) and Non-LOS (NLOS) components. Naturally, PWEs control the NLOS component only, without affecting the LOS [1]. Therefore, the following model will focus on the NLOS case. It is noted that a workaround for total control over NLOS and LOS with PWEs is discussed in Section VI.

Consider two tiles, h and h' , in a 3D space. We will consider these tiles as *connectable* if there exist any input $\widetilde{\mathbb{I}}$ and functions $f_h, f_{h'}$, such that:

$$f_h(f_h(\widetilde{\mathbb{I}})) \rightarrow \emptyset \iff f_{h'} : f_{h'}^{ABS}, \forall f_h(\widetilde{\mathbb{I}}) \neq \emptyset \quad (22)$$

In other words, inter-tile connectivity means that one tile can redirect impinging EM energy to another. It is implied that the redirected power is significant, i.e., it surpasses a practical threshold defined by the application scenario. Thus, connectability may be precluded due to physical obstacles between tiles, or by the lack of supported tile functions to redirect significant energy to one another.

Additionally, we consider a set of user devices, \mathcal{U} , in the same space. User $u \in \mathcal{U}$ will be considered *connected* to tile h if there exists any LOS input $\widetilde{\mathbb{I}}$ and a function f_h such that:

$$f_h(\widetilde{\mathbb{I}}) \rightarrow \emptyset \iff f_h : f_h^{ABS}, \forall \widetilde{\mathbb{I}} \neq \emptyset \quad (23)$$

i.e., getting zero output from a tile connected to a user is only possible if a full absorption functionality is employed.

Based on relations (22) and (23), we define the notion of:

- the set of inter-tile links, \mathcal{L}_h , where each contained link $l_{h,h'} \in \mathcal{L}_h$ denotes tile *connectivity potential* by relation (22), and
- the set of user-tile links, \mathcal{L}_u , where each contained link $l_{u,h} \in \mathcal{L}_u$ denotes *connection* by relation (23).

Following the symmetry Remark 1, all links in \mathcal{L}_h and \mathcal{L}_u are bidirectional and symmetric. Additionally all links will be considered to have an associated label, $\text{DELAY}(l)$, defined as the wave propagation delay, inclusive of any delay within the receiving end. Finally, last-tile-to-receiving-user links may be labeled as $\text{TX}(l_{u,h}) \in \mathcal{U}$, to designate the transmitting user that may employ them. Likewise, transmitting-user-to-first-tile links may be labeled as $\text{RX}(l_{u,h}) \in \mathcal{U}$, to designate the receiving user that must be reached via them. The labeling is intended to capture the Multiple-Input-Multiple-Output (MIMO) potential of the user devices at a high level.

Based on the above definitions, we proceed to define the graph $\mathcal{G}(\{\mathcal{H}, \mathcal{U}\}, \{\mathcal{L}_h, \mathcal{L}_u\})$, as well as subgraphs of the form $\mathcal{G}(\{f_h\})$. The latter represent environments that have been configured by applying specific functions to tiles, thus instantiating some of the allowed links \mathcal{L}_h . We consider an EM flow, $\langle u_{\text{TX}}, u_{\text{RX}} \rangle$, from a transmitter u_{TX} to a receiver u_{RX} , following a path via tiles within $\mathcal{G}(\{f_h\})$, defined as an ordered selection of links without repetitions:

$$\vec{p}_{\langle u_{\text{TX}}, u_{\text{RX}} \rangle} = \{l_{u_{\text{TX}}h_1}, l_{h_1h_2}, l_{h_2h_3}, \dots, l_{h_N u_{\text{RX}}}\}. \quad (24)$$

Remark 6. The above formulation with non-repeating links in paths is also posed in compliance with Remark 4, which dictates the avoidance of function combinations. To understand this claim, consider a counterexample with a repetitive path. This path must have the form $\{\dots, l_{h_k h_i}, l_{h_i h_{i+1}}, \dots, l_{h_i h_i}, l_{h_i h_{i+1}}, \dots\}$ where $k \neq l$. Due to the symmetry Remark 1, a reverse input via the repeated link $l_{h_i h_{i+1}}$ must exit from both $l_{h_k h_i}$ and $l_{h_i h_i}$. This requires a splitting function at tile h_i , which is a combined function, as described in the context of relation (19).

Any input $\widetilde{\mathbb{I}}$ at tile h_1 is transformed over the path as:

$$\widetilde{\mathbb{O}}(\widetilde{\mathbb{I}}, \vec{p}_{\langle u_{\text{TX}}, u_{\text{RX}} \rangle}) \leftarrow f_{h_N} \circ \dots \circ f_{h_3} \circ f_{h_2} \circ f_{h_1} \circ \widetilde{\mathbb{I}} \quad (25)$$

where $f_{h_j} \circ f_{h_i}$ implies passing only the output of f_{h_i} that impinges tile h_j to f_{h_j} , and ignoring any other outputs of f_{h_i} . Without loss of generality, relation (25) omits the propagation over the first and last link, which are subject to antenna characteristics and standard (non-programmable) propagation. The end-to-end delay of a path can be calculated in a trivial manner as the sum of all link delays:

$$\text{DELAY}(\vec{p}_{\langle u_{\text{TX}}, u_{\text{RX}} \rangle}) = \sum_{\forall l \in \vec{p}} \text{DELAY}(l) \quad (26)$$

We proceed to consider all paths that reach the receiver u_{RX} , from any transmitter $(*)$ (noting the possible multiplicity of paths for the same $\langle u_{\text{TX}}, u_{\text{RX}} \rangle$ pair). The total received output is then:

$$\widetilde{\mathbb{O}}_{u_{\text{RX}}}^{\text{TOTAL}} = \sum_{\forall \vec{p} : \vec{p} \langle *, u_{\text{RX}} \rangle} \widetilde{\mathbb{O}}(\widetilde{\mathbb{I}}, \vec{p}) \quad (27)$$

Relations (26), (27) contain all the required information for deriving the communication quality of a pair $\langle u_{\text{TX}}, u_{\text{RX}} \rangle$. Moreover, due to the symmetry Remark 1, the derivations of relations (26), (27) are identical for the reverse path, $\langle u_{\text{RX}}, u_{\text{TX}} \rangle$. Finally, the labeling $\text{TX}(l_{h_N u_{\text{RX}}})$ of the receiver's links can be employed to classify outputs as useful or interfering based on the MIMO configuration.

The paths $\vec{p}_{\langle u_{\text{TX}}, u_{\text{RX}} \rangle}$ are directly derived from the deployed tile functions and the corresponding graph $\mathcal{G}(\{f_h\})$. The simulated NLOS propagation procedure is modeled as NLOSPROP (Algorithm 1). The process receives as inputs: i) the configured tiles, ii) a receiver, and iii) all transmitting users and their inputs ($\widetilde{\mathbb{I}}$ for each link connecting the transmitter to a tile). The process produces the paths leading from any transmitter to the receiver. Internally, a tuple denoted as *ray* is used for holding a path (cf. rel. (24)) and its input. A stack of *rays* is initialized per transmitter link (lines 3–6). The model then continuously updates each ray, accounting for tile interactions (line 9). It is

Algorithm 1 Simulated NLOS propagation model for PWEs.

```

1: procedure  $\text{PATHS}_{\text{RX}}$ :  $\text{NLOSPROP}(\mathcal{G}(\{f_h\}), u_{\text{RX}},$ 
    $\left\{ \left\langle u_{\text{TX}}, \left\{ \tilde{\mathbb{I}}_h, h : l_{u,h} \in \{\mathcal{L}_u : u = u_{\text{TX}}\} \right\} \right\rangle \right\}$ )
2:    $\text{rays} \leftarrow \{\}, \text{PATHS}_{\text{RX}} \leftarrow \{\}$ ;
3:   for  $l_{u,h} \in \{\mathcal{L}_u : u \in \{u_{\text{TX}}\}\}$  //for all transmitters.
4:      $r \leftarrow \left\langle \vec{p}_r = \{l_{u,h}\}, \tilde{\mathbb{I}}_r = \tilde{\mathbb{I}}_h \right\rangle$ ;
5:      $\text{rays} \leftarrow \text{rays} + r$ ;
6:   end for
7:   while  $\text{rays} \neq \emptyset$ 
8:      $r \leftarrow \text{rays.pop}()$ ; //remove and return last entry.
9:     for  $o \in \tilde{\mathbb{O}}(r : \tilde{\mathbb{I}}_r, r : \vec{p}_r)$  //cf. rel. (25).
10:       $h^* \leftarrow \text{TILE\_REACHED}(o)$ ; //cf. rel. (22).
11:       $u^* \leftarrow \text{USER\_REACHED}(o)$ ; //cf. rel. (23).
12:       $h \leftarrow \text{LAST\_TILE}(r : \vec{p}_r)$ ;
13:      if ( $u^* = u_{\text{RX}}$ )
14:         $r^* \leftarrow \left\langle r : \vec{p}_r + l_{h,u^*}, r : \tilde{\mathbb{I}}_r \right\rangle$ ;
15:         $\text{PATHS}_{\text{RX}} \leftarrow \text{PATHS}_{\text{RX}} + (r : \vec{p}_r + l_{h,u^*})$ ;
16:      else if ( $h^* \neq \emptyset$ )
17:         $r^* \leftarrow \left\langle r : \vec{p}_r + l_{h,h^*}, r : \tilde{\mathbb{I}}_r \right\rangle$ ;
18:         $\text{rays} \leftarrow \text{rays} + r^*$ ;
19:      end if
20:    end for
21:  end while

```

noted that each interaction may yield more than one outputs. Once a path reaches the intended user, it is added to the model outputs (lines 13–15) and the corresponding ray is discarded. If a tile is reached, a copy of the ray with an updated path is added to the ray set for further processing (lines 16–19). The model accounts for attenuated rays, by using the connectivity definitions (22), (23)–weak rays are treated as null outputs. Furthermore, notice that rays escaping the consider space are discarded as expected (lines 10,11 will yield null outputs). Finally, notice that the model can also provide the paths to a set of receivers, $\{u_{\text{RX}}\}$, by modifying the condition in line 13 as $u^* \in \{u_{\text{RX}}\}$.

Remark 7. Programmable wireless environments seek to optimize the communication for any set $\langle \{u_{\text{RX}}\}, \{u_{\text{TX}}\} \rangle$, by deploying the corresponding, performance optimizing tile functions. This can be generally formulated as:

$$\{f_h\}^{OPT} \leftarrow \arg \text{opt}(\text{OBJECTIVE}(\text{LOSPROP}(\langle \{u_{\text{RX}}\}, \{u_{\text{TX}}\} \rangle), \{f_h\}) + \text{NLOSPROP}(\mathcal{G}(\{f_h\}), \langle \{u_{\text{RX}}\}, \{u_{\text{TX}}\} \rangle))) \quad (28)$$

where OBJECTIVE is a fitness function applied to the propagation outcome, and the inputs $\tilde{\mathbb{I}}$ of NLOSPROP are omitted for clarity. The OBJECTIVE may freely refer to:

- 1 transmitter to 1 receiver (uni-cast), $\langle u_{\text{TX}}, u_{\text{RX}} \rangle$,
- 1 transmitter to many receivers (multi-cast or broad-cast), $\langle u_{\text{TX}}, \{u_{\text{RX}}\} \rangle$,
- many transmitters to many receivers, $\langle \{u_{\text{TX}}\}, \{u_{\text{RX}}\} \rangle$.

The latter two categories inherently incorporate resource sharing policies among communicating pairs.

It is noted that the formulation of relation (28) is generic and, thus, also covers cases that are not compliant to Remark 4 about tile functionality reuse.

E. Modeling connectivity objectives

We proceed to study specific objectives for core aspects of wireless system performance. We focus on objectives pertaining to a single receiver, since resource sharing policies are subjective. It is noted, however, that Section IV case-studies the integration of objectives and policies. Additionally, all LOS components will be omitted for clarity, since they are either not affected by PWEs or be manipulated for control in the same manner as NLOS, as described later in Section VI.

We proceed to define a path-centric formulation for various core objectives. In other words, we employ the correspondence $\{f_h\} \leftrightarrow \vec{p}$ between a set of deployed functions f_h and formed paths \vec{p} interconnecting the various users within the PWE. The practicality of this choice will be explained in the remainder of the current subsection and in Section IV.

Power transfer maximization.: We study the objective of maximizing the total power received by a specific user, emitted by a group of transmitters. This objective is practical for wireless power transfer [1], as well as for formulating subsequent objectives. Using a path-centric approach, relation (28) can be rewritten as:

$$\{\vec{p}\} \stackrel{OPT}{\leftarrow} \arg \max_{\{\vec{p}\}} \left(\sum_{\forall u^* \in \{u_{\text{TX}}\}} \sum_{\forall i} \tilde{\mathbb{O}}(\tilde{\mathbb{I}}_{u^*,i}, \vec{p}_i^{\langle u^*, u_{\text{RX}} \rangle}) \right) \quad (29)$$

I.e., the maximization of the aggregate output of all paths leading to the studied receiver, u_{RX} , where i indexes multiple paths for the same transmitter-receiver pair. Since the objective is the maximization of power, only the \mathbf{P} attribute of $\tilde{\mathbb{O}}$ needs to be retained (cf. def. (6), (8)). Moreover, the output can be expressed as the product of all gain metrics g_h (defined in Section III-C) over the tiles comprising each path, multiplied by the input power of the path:

$$\{\vec{p}\} \stackrel{OPT}{\leftarrow} \arg \max_{\{\vec{p}\}} \left(\sum_{\forall u^* \in \{u_{\text{TX}}\}} \sum_{\forall i} \mathbf{P}_{u^*,i} \cdot \prod_{\forall h \in \vec{p}_i^{\langle u^*, u_{\text{RX}} \rangle}} g_h \right) \quad (30)$$

It is noted that the path-centric formulation allows for the employing the $\prod g_h$ expression in relation (30). In other words, treating a path as input to the optimization, allows for calculating (and caching) its total effect on the transmitter power. An alternative f_h -centric formulation would not allow this simple expression, since the output of a tile—and, thus, its gain—depends on the input wave and the deployed tile function (e.g., cf. rel.(13)). Thus, a function-centric formulation would have to follow expression (25), where each gain would receive as input the preceding gains and be passed as argument to the next one, i.e., $g(g(g(\dots)))$.

QoS optimization.: QoS refers to optimizing some aspect of the communication channel between two users. Without loss of generality, we will focus on the maximization of the useful-signal-to-interference ratio (\mathbf{P}^{TOT}/I) at the studied receiver, u_{RX} . The useful received signal is expressed as:

$$\mathbf{P}^{TOT} = \sum_{\forall u^* \in \{u_{TX}\}} \sum_{\forall i} \mathbf{P}_{u^*,i} \cdot \prod_{\forall h \in \vec{p}_i^{u^*,u_{RX}} : \mathcal{P}} g_h \quad (31)$$

where

$$\mathcal{P}' : \{ \vec{p}_i^{u^*,u_{RX}} \in \mathcal{P} \mid \text{DELAY}(\vec{p}_i^{u^*,u_{RX}}) - \min(\{\text{DELAY}(\vec{p}' \in \mathcal{P})\}) < D_{TH} \} \quad (32)$$

$$\mathcal{P} : \{ \vec{p}_i^{u^*,u_{RX}} \mid \text{TX}(\text{LASTLINK}(\vec{p}_i^{u^*,u_{RX}})) = u^*, \text{RX}(\text{FIRSTLINK}(\vec{p}_i^{u^*,u_{RX}})) = u_{RX} \} \quad (33)$$

Restriction (33) (defining path set \mathcal{P}) states that a path carries useful signal : i) if the transmission is intended for the studied receiver, and ii) is received by a link labeled to expect the transmitter emission. Therefore, it is implied that the MIMO capabilities of the user devices have also been configured. (This is accomplished in Section IV). Restriction (32) defines a subset of \mathcal{P} , based on the latency of each path. Accounting for constructive signal superposition, the selected paths carrying useful signal must have bounded latency (i.e., within a time window defined by the fastest path, plus an application-specific threshold value D_{TH}).

The interference is expressed similarly to \mathbf{P}^{TOT} but over all paths \mathcal{P}' leading to the studied receiver, but not found in \mathcal{P}' :

$$\mathbf{I} = \sum_{\forall u^* \in \{u_{TX}\}} \sum_{\forall i} \mathbf{P}_{u^*,i} \cdot \prod_{\forall h \in \vec{p}_i^{u^*,u_{RX}} : \mathcal{P}'} g_h \quad (34)$$

Finally, the QoS optimization objective is expressed as:

$$\{ \vec{p} \} \stackrel{OPT}{\leftarrow} \arg \max_{\{ \vec{p} \}} \left(\frac{\mathbf{P}^{TOT}}{\mathbf{I}} \right) \quad (35)$$

Eavesdropping mitigation.: Security concerns pertaining to eavesdropping can be taken into account and be combined with other objectives [6]. Eavesdropping mitigation is achieved by ensuring that the employed communication paths avoid all but the intended user. To this end, consider a 3D surface, $S(u)$, around a user u . $S(u)$ can exemplarily be a sphere centered at the user's position. We proceed to discard the paths produced by Algorithm 1 that geometrically intersect with the $S(u)$ (i.e., a check for intersection between any link in the path and the surface). Avoiding any user but the intended receiver can then be expressed as:

$$\vec{p}_i^{u^*,u_{RX}} \mid \vec{p}_i \cap S(u) \rightarrow \emptyset, \forall u \neq u_{RX}, u \in \mathcal{U} \quad (36)$$

Restriction (36) can be further customized, e.g., to avoid a targeted set of users only, to discard paths prone to eavesdropping based on the intersection with some convex hull surface covering many users, or even to quantify the eavesdropping risk as a scalar value, such as the minimum distance between a path and a user device.

The expression of a security concern as a restriction over paths, allows for natural combination between security and QoS or power transfer objectives. Restriction (36) can simply filter out paths before \mathcal{P} (restriction (33)) or after \mathcal{P}' (restriction (32)). In the former case security is prioritized over connectivity, while in the latter case connectivity comes first.

Remark 8. The described eavesdropping mitigation approach naturally limits the interference caused to unintended recipients. Thus, the eavesdropping mitigation is not antagonistic to other QoS objectives.

Doppler effect mitigation: The geometric approach in path restrictions can be extended to mitigate Doppler effects. Frequency shifts owed to Doppler effects are especially important in mm-wave communications (and higher frequencies), where even pedestrian movement rapidly deteriorates the reception quality [27]. To this end, PWE can strive to keep the last link of communication paths perpendicular to the trajectory of the user, $\vec{m}_{u_{RX}}$, as follows:

$$\vec{p}_i^{u^*,u_{RX}} \mid \text{LASTLINK}(\vec{p}_i) \perp \vec{m}_{u_{RX}} \quad (37)$$

Restriction (37) can alternatively be relaxed to a scalar metric of perpendicularity, e.g., as the inner product of the unary vector across $\text{LASTLINK}(\vec{p}_i)$ and the unary derivative of $\vec{m}_{u_{RX}}$ at the user position. Finally, restriction (37) can be combined with all preceding objectives in a manner identical to the eavesdropping case.

User blocking: Blocking a user from gaining access to another device, such as an access point, can be facilitated by configuring a PWE to absorb its NLOS emissions. In this manner, potential security risks can be mitigated at the physical layer, before expending resources for blocking them at a higher level (e.g., MAC slots, software authorization steps) [1], [6], [13]. The mathematical formulation follows naturally from relation (30), by replacing \max with \min within the objective. It is implied that information on user authorization is passed to the PWE configuration as an input.

Finally, it is noted that this objective needs *not* be combined with any other, given that it intends to fully block the physical connectivity of a user, rather than assign resources to him.

IV. A K-PATHS APPROACH FOR MULTI-USER MULTI-OBJECTIVE ENVIRONMENT CONFIGURATION

The preceding Section formulated the PWE configuration objectives, using graph paths as inputs. We proceed to define the KPCONFIG heuristic, which configures a PWE for serving a set of user objectives (Algorithm 2). KPCONFIG receives the following input parameters:

- The PWE graph \mathcal{G} comprising the sub-graphs of connected users, $\mathcal{G}(\mathcal{U}, \mathcal{L}_u)$, and connectable tiles, $\mathcal{G}(\mathcal{H}, \mathcal{L}_h)$. We consider the latter as static and, therefore, pre-processable. Particularly, we assume that a custom number of node-disjoint shortest paths can be pre-calculated and cached, for each tile pair. The link weight for such calculations is the link DELAY, and the ensuing paths are considered to be filtered based on their total steering gain (cf. the $\prod g_h$ expression in relation (30)) and a custom acceptable threshold. Subsequent calls to well-known path finding algorithms (e.g., SHORTESTPATH, KSHORTESTPATHS [28]) are considered to be executed on top of this cache.
- The set of communicating user pairs and their objectives. Multicast groups are expressed as multiple pairs with the same transmitter. The objective OBJ is a set of binary

Algorithm 2 The K-Paths approach for configuring PWEs.

```

1: procedure KPCONFIG( $\mathcal{G}, \{\langle u_{TX}, u_{RX}, OBJ \rangle\}$ ),
    $\{\langle u_{TX}, \{\tilde{\mathbb{I}}_h, h : l_{u,h} \in \{\mathcal{L}_u : u = u_{TX}\}\} \rangle\}$ 
2:    $blocked\_pairs, sorted\_pairs, N_e, K_e \leftarrow$  MDFPOLICY(
    $\mathcal{G}, \{\langle u_{TX}, u_{RX}, OBJ \rangle\}$ );
3:    $paths\_rem \leftarrow 0$ ;
4:   for  $e : \langle u_{TX}, u_{RX}, OBJ \rangle$  in  $sorted\_pairs$ 
5:      $paths \leftarrow \{\emptyset\}$ ;
6:     for  $i = 1 : 1 : K_e$ 
7:        $\mathcal{L}_a \leftarrow$  FILTERLINKSBYOBJ( $\mathcal{G}, OBJ$ );
8:        $\vec{p} \leftarrow$  FINDCOMPLEXPATH( $\mathcal{G}, u_{TX}, u_{RX}, \mathcal{L}_a, paths$ );
9:       if  $\vec{p} = \emptyset$ 
10:        break;
11:       end if
12:        $paths \leftarrow paths + \vec{p}$ ;
13:     end for
14:     if  $\|paths\| = 0$ 
15:       continue; //pair is disconnected.
16:     end
17:      $max\_paths \leftarrow \min \{N_e + paths\_rem, \|paths\|\}$ ;
18:      $paths \leftarrow$  FILTERPATHSBYOBJ( $paths, max\_paths, OBJ$ );
19:      $paths\_rem \leftarrow paths\_rem + \max \{max\_paths - \|paths\|, 0\}$ ;
20:     DEPLOY( $\mathcal{G}, paths$ );
21:   end for
22:   DEPLOYBLOCKS( $\mathcal{G}, blocked\_pairs$ );
23:    $f_h \leftarrow f_h^{ABS}, \forall h \in \mathcal{G} : f_h = \emptyset$ ;

```

flags, each denoting a type from Section III-E. We assume that symmetric pairs have been filtered out of this parameter. Complimenting Remark 1, a pair $\langle u_{TX}, u_{RX}, OBJ \rangle$ is symmetric to $\langle u_{RX}, u_{TX}, OBJ \rangle$, highlighting that the objective must also be the same. Moreover, disconnected pairs (i.e., without any SHORTESTPATH in \mathcal{G}) are also considered as filtered out.

- The inputs $\tilde{\mathbb{I}}_h$ and the affected tiles, for each transmitter.

The use of the link DELAY as the link weight prioritizes shorter links to assemble a path. In practice, the output of a tile function may digress from the intended as the distance from the tile increases [2], [17]. In this aspect, shorter links may favor a more consistent behavior. Additionally, the output of KPCONFIG is a set of paths per pair (which correspond to tile functions as described in Section III-E). Thus, the TX and RX labels per user link are naturally produced by KPCONFIG, without further steps.

Since KPCONFIG seeks to serve multiple user pairs, a resource sharing policy needs to be employed in the general case. Thus, at line 2, KPCONFIG, calls upon the 'Most-Distant-First' (MDFPOLICY) subroutine, which is an exemplary policy.

MDFPOLICY, formulated as Algorithm 3, primarily returns a sorting of the user pairs ($sorted_pairs$) by descending priority order, as well as the number of paths to allocate per pair e , N_e . At lines 9 – 21, MDFPOLICY filters out any pairs with user access BLOCK objectives, since these will not require connecting paths. Remaining pairs are sorted by descending average delay, calculated over K_e shortest paths in graph \mathcal{G} , K_e being the minimum number of user links in the pair e .

Algorithm 3 The ‘‘Most Distant Pair First’’ resource sharing policy for PWEs.

```

1: procedure blocked_pairs, sorted_pairs,  $N_e, K_e$ :
2: MDFPOLICY( $\mathcal{G}, \{\langle u_{TX}, u_{RX}, OBJ \rangle\}$ )
3:    $n_u \leftarrow \{0, \dots, 0\}$ ; //for all users.
4:    $sorted\_pairs \leftarrow \{\emptyset\}$ ;
5:    $blocked\_pairs \leftarrow \{\emptyset\}$ ;
6:    $v_e \leftarrow \{\emptyset\}$ ;
7:    $K_e \leftarrow \{\emptyset\}$ ;
8:    $N_e \leftarrow \{\emptyset\}$ ;
9:   for  $e : \langle u_{TX}, u_{RX}, OBJ \rangle$  in  $\{\langle u_{TX}, u_{RX}, OBJ \rangle\}$ 
10:    if OBJ = BLOCK //  $u_{RX}$  is arbitrary.
11:       $blocked\_pairs \leftarrow blocked\_pairs + e$ ;
12:    continue;
13:    else;
14:       $sorted\_pairs \leftarrow sorted\_pairs + e$ ;
15:    end if
16:     $K_e \leftarrow \min \{\|\mathcal{L}_{u:u_{TX}}\|, \|\mathcal{L}_{u:u_{RX}}\|\}$ ;
17:     $\{\vec{p}\}_e \leftarrow$  KSHORTESTPATHS( $\mathcal{G}, K_e, u_{TX}, u_{RX}$ );
18:     $v_e \leftarrow$  MEAN( $\{\text{DELAY}(\vec{p})\}_e$ );
19:     $n_{u_{TX}} \leftarrow n_{u_{TX}} + \|\{\vec{p}\}_e\|$ ;
20:     $n_{u_{RX}} \leftarrow n_{u_{RX}} + \|\{\vec{p}\}_e\|$ ;
21:  end for
22:   $sorted\_pairs \leftarrow$  SORTDESC( $sorted\_pairs, v_e$ );
23:  for  $e : \langle u_{TX}, u_{RX}, OBJ \rangle$  in  $sorted\_pairs$ 
24:     $N_e \leftarrow \max \left\{ \min \left\{ \left\lfloor \frac{\|\mathcal{L}_{u:u_{TX}}\|}{n_{u_{TX}}} \right\rfloor, \left\lfloor \frac{\|\mathcal{L}_{u:u_{RX}}\|}{n_{u_{RX}}} \right\rfloor \right\}, 1 \right\}$ ;
25:  end for

```

Algorithm 4 Obtaining links in conflict with eavesdropping and Doppler effect mitigation objectives.

```

1: procedure  $\mathcal{L}_a : \text{FILTERLINKSBYOBJ}(\mathcal{G}, OBJ)$ 
2:    $\mathcal{L}_a \leftarrow \{\}$ ;
3:   switch OBJ:
4:     case MITIGATEEAVESDROP: //Inputs of (36) implied.
5:        $\mathcal{L}_a \leftarrow \mathcal{L}_a + \text{relation (36)}$ ;
6:     case MITIGATEDOPPLER: //Inputs of (37) implied.
7:        $\mathcal{L}_a \leftarrow \mathcal{L}_a + \text{relation (37)}$ ;
8:   end switch

```

This simple heuristic intends to prioritize distant pairs, on the grounds of experiencing a lesser degree of propagation control. Finally, the tentative number of paths, N_e , to allocate pair pair is returned at line 24, as the minimum ratio of number of user links divided by the number of pairs this user belongs to.

KPCONFIG (Algorithm 2) then resumes its operation. In general, it comprises an exploratory evaluation of K_e paths per sorted pair (lines 6 – 13), eventually keeping and deploying at most N_e subject to compliance with objectives (lines 17 – 20). Left-over path allocations are redistributed to ensuing pairs via the $paths_rem$ variable (lines 3, 19).

The exploration of K_e paths at lines 6 – 13 is also a point for enforcing eavesdropping and Doppler effect mitigation objective types. At line 7, the FILTERLINKSBYOBJ subroutine is called (Algorithm 4), which returns the links \mathcal{L}_a of \mathcal{G} that are in conflict with the objectives. The use of switch without break statements implies that both objectives can be active for the same user pair.

Algorithm 5 The process for finding a single path in a PWE.

```

1: procedure  $\vec{p}$ : FINDCOMPLEXPATH(
    $\mathcal{G}, u_{TX}, u_{RX}, \mathcal{L}_a, paths$ )
2:  $\mathcal{G}' \leftarrow \mathcal{G} \setminus \{\mathcal{H}, u_{TX}, u_{RX}\}, \{\mathcal{L}_h, \mathcal{L}_{u_{TX}}, \mathcal{L}_{u_{RX}}\} - \mathcal{L}_a - paths$ ;
3:  $\mathcal{G}^* \leftarrow \mathcal{G}' - \langle \mathcal{H} | f_h = \emptyset \rangle$ ;
4:  $\vec{p} \leftarrow \text{SHORTESTPATH}(\mathcal{G}^*, u_{TX}, u_{RX})$ ;
5: if  $\vec{p} \neq \emptyset$ 
6:   return  $\vec{p}$ ; //Path without deployed functions found.
7: end if
8:  $\vec{p}^* \leftarrow \text{SHORTESTPATH}(\mathcal{G}', u_{TX}, u_{RX})$ ;
9: if  $\vec{p}^* = \emptyset$ 
10:  return  $\emptyset$ ; //No path exists
11: end if
12:  $\vec{p} \leftarrow \{\}$ ;  $h' \leftarrow \emptyset$ ;
13: for  $\langle l, h \rangle$  in  $\vec{p}^*$ 
14:  if  $f_h = \emptyset$ 
15:    $\vec{p} \leftarrow \vec{p} + l$ ;
16:  else
17:    $\langle l', h' \rangle \leftarrow f_h(l)$ ;
18:    $\vec{p} \leftarrow \vec{p} + l'$ ;
19:  break;
20: end if
21: end for
22:  $\vec{p}^* \leftarrow \text{SELF}(\mathcal{G}, h', u_{RX}, \mathcal{L}_a, paths - \vec{p})$ ;
23: if  $\vec{p}^* = \emptyset$ 
24:  return  $\emptyset$ ;
25: else
26:  return  $\vec{p} + \vec{p}^*$ ;
27: end if

```

At line 7 of KPCONFIG (Algorithm 2), the links \mathcal{L}_a are passed to the FINDCOMPLEXPATH subroutine (Algorithm 5), which seeks to find a path in \mathcal{G} that connects the pair while avoiding the links \mathcal{L}_a and the links over the already deployed $paths$. Two subgraphs are created at lines 2 and 3 of Algorithm 5. The subgraph \mathcal{G}' , which removes the aforementioned links from the original graph \mathcal{G} , and \mathcal{G}^* which also removes the already configured tiles (nodes) of \mathcal{G}' . FINDCOMPLEXPATH first tries to find a connecting path in \mathcal{G}^* (line 4). If found, the path comprises unconfigured tiles only, thus being in compliance with Remark 4 and avoiding the combination of tile functions. If not found, the search continues on \mathcal{G}' . A found path is then bound to contain already configured tiles. Lines 13–21 iterate over the path links and tiles until the first configured tile is found (lines 16–20). Then, the output (link l' and reached tile h') of the already deployed function are calculated (line 17). The subroutine is then recursively called to find a path from h' to the intended receiver, while also avoiding links already visited.

Returning to the workflow of KPCONFIG (Algorithm 2), line 17 is reached with a maximum of K_e found paths that have remained from preceding pairs (line 17), an objective-driven selection of paths takes place at line 18 via the FILTERPATHS-BYOBJ subroutine (Algorithm 6).

FILTERPATHS-BYOBJ considers a power maximization or a QoS optimization objective, since these cannot be generally

Algorithm 6 Objective-oriented propagation path selection.

```

1: procedure  $sel\_paths$ :
2: FILTERPATHS-BYOBJ( $paths, max\_paths, OBJ$ )
3: switch OBJ
4:  case MAXPOWER: //Inputs of (30) implied.
5:    $paths \leftarrow \text{SORTDESC}(paths)$ ; // by  $P \cdot \prod g_h$ .
6:    $paths \leftarrow \text{KEEPTOPN}(paths, max\_paths)$ ;
7:   break;
8:  case MAXSIR: //Inputs of (31) implied.
9:    $paths \leftarrow \text{SORTASC}(paths)$ ; // by path DELAY.
10:  for  $i=1:1:\|paths\|$ 
11:    $P_i^{TOT} \leftarrow$  //by rel. (31),(32).
12:    $P_i^{TOT}(paths_{i, \min\{i+max\_paths, \|paths\|\}})$ 
13:  end for
14:   $i^{OPT} \leftarrow \arg \max \{P_i^{TOT}\}$ ;
15:   $paths_{i^{OPT}, \min\{i^{OPT}+max\_paths, \|paths\|\}}$ ;
16:  break;
17: end switch
18:  $sel\_paths \leftarrow paths$ ;

```

Algorithm 7 The process for blocking user access in PWE.

```

1: procedure DEPLOYBLOCKS( $\mathcal{G}, blocked\_pairs$ )
2: for  $e : \langle u_{TX}, u_{RX}, OBJ \rangle$  in  $blocked\_pairs$ 
3:  for  $l_{u, h^*} \in \mathcal{L}_u | u = u_{TX}$ 
4:    $\vec{p} \leftarrow \text{FINDCOMPLEXPATH}(\mathcal{G}, h^*, u_{RX})$ ;
5:   for  $h \in \vec{p}$ 
6:    if  $f_h = \emptyset$ 
7:      $f_h \leftarrow f_h^{ABS}$ ;
8:    break;
9:   end if
10:  end for
11: end for
12: end for

```

combined. The path selection for power transfer maximization is straightforward: the paths are sorted by total power and the top ones are selected. For a QoS optimization, the paths are first order by total delay. Then, a sliding window-based selection takes place, keeping the path subset that maximizes relation (31) subject to (32). Notice this approach does not take into account the signal interference (relation (34)). Instead, an eavesdropping objective can be added to all user pairs, thus naturally minimizing or mitigating interference as well.

KPCONFIG (Algorithm 2) proceeds to DEPLOY the selected paths at line 20, updating the f_h status in \mathcal{G} as well. The deployment takes place by setting collimation functions, f_h^{COL} , at the first and last tile of the path, and steering functions, f_h^{STR} , to intermediate ones. Already configured tiles are not affected. Required modifiers, m_h^{PHA} or m_h^{POL} are applied afterwards sequentially, at the tile that yields the smallest effect on the total path gain $\prod g$. At line 22, KPCONFIG (Algorithm 2) takes action to block unauthorized users, contained in the $blocked_pairs$ set. The process is given in the subroutine DEPLOYBLOCKS (Algorithm 7). Since the objective is to block a single user from all others, we proceed to iterate over the user links of u_{TX} and fully absorb the emissions at each one. Notice that the immediately affected tiles may have a

deployed function. Thus, in the general case, DEPLOYBLOCKS searches for a path from u_{TX} to an arbitrary node (random user u_{RX} or any random tile). Once found, the path is iterated over and a full absorption function, f_h^{ABS} , is deployed at the first unconfigured tile h .

Finally, KPCONFIG (Algorithm 2) concludes at line 23 by setting all unused tiles in \mathcal{G} to absorb from an arbitrary direction (e.g., from the tile surface normal). Thus, parasitic function outputs within PWE can be attenuated. It is noted that this step can be omitted, e.g., in cases where limiting the total number of configured tiles is a concern.

V. EVALUATION

We proceed to evaluate the performance of KPCONFIG in a set of floorplans, users and objectives. We seek to demonstrate and visualize compliance to performance objectives, and deduce the performance gains in comparison with natural propagation (non-PWE).

The evaluation is based on a novel tool, implementing the process described in Section III, developed specifically for simulating PWEs. The tool receives a floorplan, a set of configured tiles, as well as users locations and user transmission characteristics. Subsequently, it essentially executes the process of Algorithm 1. Its simulation output is the power-delay profile for each user, which is then used for quantifying the compliance with the set objectives. The tool is implemented in JAVA over the AnyLogic platform [29]. The latter is chosen due to its strong visualization capabilities, and its versatility in combining simulation models (discrete events, agents, continuous processes) to describe a complex system. The developed tool, freely available on demand, allows for realistic simulation of PWE, supporting the following features:

- Using any EM tile profile as input, supporting any physical implementation approach. The EM profiles can be input from Computational EM packages, or real measurements in a well-defined format.
- Customized antenna radiation patterns with MIMO support.
- Allowing for controllable reflection, refraction and diffraction of EM waves, along with any described meta-surface functionality.
- Flexible scenario creation via a 3D Graphical User Interface, allowing for varying tile topologies, dimensions, floorplan, user placement and roles, user mobility trajectories, and partially coated environments.
- Flexible user objective definition mechanism, readily supporting all described objectives and allowing for creating custom ones.
- Multi-cast and broadcast support.
- Script-able and automate-able, parallelized simulations, allowing for automated parameter optimization, parameter sensitivity, Monte Carlo experiments, and general-purpose heuristic optimization runs [29].

Table III summarizes the persistent parameters across all subsequent tests. The following notes are made:

- The user positions and radiation characteristics are considered to be known. These can be deduced by a user

TABLE III
PERSISTENT SIMULATION PARAMETERS.

Ceiling Height	3 m
Tile Dimensions	1×1 m
Tile Functions	f_h^{COL} , f_h^{STR} , f_h^{ABS}
Non-HSF surfaces	Perfect reflectors
User scattering model	Blocking spheres, radius 0.5 m
Frequency	2.4 GHz
Tx Power	-30 dBm
Antenna type	Single a° -lobe sinusoid, pointing at ϕ°, θ° (cf. Fig. 6)
Max ray bounces	50
Min considered ray power	-250 dBm

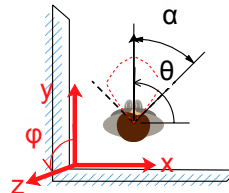


Fig. 6. User location and beam orientation coordinate system. The origin is at the lower left corner of each floorplan.

localization scheme specific for PWEs [21], or a third party scheme.

- All tiles have the same EM profile (cf. Remark 5), which is defined as follows: all impinging waves are attenuated by a constant factor of $g = 1\%$ of the carried power, for any type of deployed function. While simplified, this profile can represent existing EM models [17], when the meta-atom resolution is infinite [30].
- The considered tile functionalities include collimation, steering and absorption, while modifiers are not taken into account. As previously described, collimation is the effect of aligning EM waves to propagate over a flat front, rather than to dissipate over an ever-growing sphere. Thus, the path loss between two tiles in a PWE is not subject to the $\propto 1/d^2$ rule, d being their distance (cf. Fig. 4) [6]. This rule is only valid for the first impact, i.e., from the transmitter to its LOS tiles. The antenna aperture effect and gain are taken into account as usual.
- The antenna patterns of the transmitter and the receiver are simplified as single-lobe sinusoids, with the characteristics and θ , ϕ orientation shown in Fig. 6 and Table III. In some scenarios, we assume that the mobile devices have beamforming capabilities and are able to turn the antenna lobe towards the ceiling, in conjunction with the mobile devices' gyroscopes.

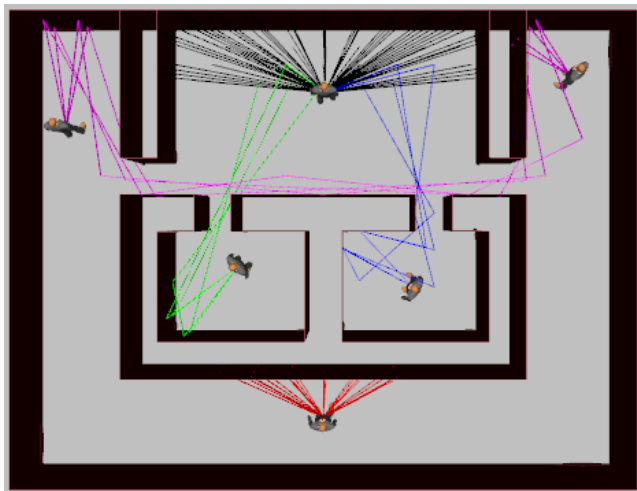
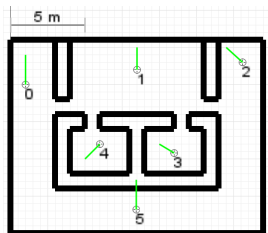
Finally, all walls, ceilings and floors are considered as fully coated with HyperSurfaces, unless otherwise stated (defined per case).

A. Multi-User Multi-Objective Showcase

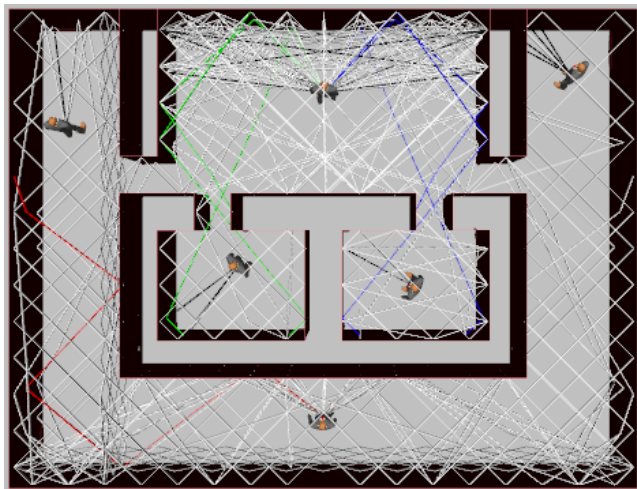
This scenario showcases the PWE performance for three communicating pairs and one unauthorized user in a floorplan, as described Table IV. The pairs have various different

TABLE IV
SCENARIO SETUP FOR THE MULTI-USER MULTI-OBJECTIVE SHOWCASE.

USER: POSITION, α, ϕ	
0:	[1.0,10.0,1.0],10.0°,0°
1:	[8.5,11.0,1.0],80.0°,0°
2:	[15.6,11.5,1.0],10.0°,0°
3:	[11.0,5.4,1.0],10.0°,0°
4:	[6.0,6.0,1.0],10.0°,0°
5:	[8.5,1.6,1.0],60.0°,0°
PAIR: OBJECTIVE	
0→2 :	MAXPOWER,EAVESMIT[[ALL]]
1→3 :	MAXPOWER,EAVESMIT[[ALL]]
1→4 :	MAXSIR,EAVESMIT[[ALL]]
5→×	BLOCK



(a) PWE



(b) No PWE

Fig. 7. Propagation with and without PWE.

objectives, while there is also a multicast group (1 to 3, 4). Moreover, the antenna characteristics vary across the users.

The achieved wireless propagation, with and without PWE, is illustrated in Fig. 7. The PWE, configured via the proposed KPCONFIG, customizes the EM propagation to uphold all objectives (Fig. 7a). Specifically, the propagation for pair 0 → 2 follows a short route within the floorplan, to achieve

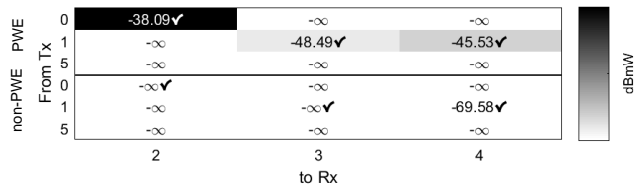
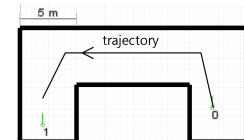


Fig. 8. Comparative power reception with and without PWE. ✓ denotes intended pair connectivity.

TABLE V
SCENARIO SETUP FOR THE DOPPLER EFFECT MITIGATION SHOWCASE.

USER: POSITION, α, ϕ	
0:	[17.0,3.2,1.0],30.0°,90.0°
1:	[2.0,1.7,1.0],30.0°,90.0°
PAIR: OBJECTIVE	
1→0 :	{MAXPOWER,EAVMIT[[0]], DOPPLERMIT[trajectory]}



maximal received power, while also avoiding all potential eavesdroppers. The pair 1 → 3 is treated similarly, i.e., maximizing the received power without QoS concerns stemming from the length of each ray. For the pair 1 → 4, however, QoS is taken into account, resulting into a selection of rays that have similar total length, as shown in Fig. 7a. Notice that, once the multicast group is served, the environment is tuned to absorb all unemployed emissions from user 1 (black lines). Finally, user 5 has its EM emissions absorbed, and is thus blocked from accessing all other users.

Natural propagation (i.e., non-PWE) within the same floorplan is shown in Fig. 7b. While some pairs achieve a degree of connectivity (e.g., 1 → 4), the propagation is expectedly chaotic. The white lines denote stray rays within the floorplan, which eventually attenuate and disappear without reaching a user. Notice that the floorplan design, coupled with the highly directional antenna lobes of some users (e.g., $\alpha = 10^\circ$) naturally secludes users and hinders connectivity.

The received power levels are shown in Fig. 8. PWE achieves objective-compliant connectivity with a relatively small loss, ranging from ~ 8 to 15 dBmW. On the other hand, the non-PWE case achieves connectivity only for pair 1 → 4, with a considerably high loss of ~ 30 dBmW. It is noted that the PWE results of Fig. 8 are calculated as the total-power-minus-interference. The classification of a ray as interfering factors for the MIMO labeling of the user links produced by KPCONFIG. (The interference was zero in all cases). In the non-PWE case, the interference classification does not consider any MIMO labeling, since there is not automatic way of setting it.

B. Doppler Effect Mitigation Showcase

We proceed to examine the mitigation of Doppler Effects, using the setup described in Table V. Both users have their antennas pointing upwards (i.e., $\phi = 90^\circ$). User 0 moves along a trajectory, and KPCONFIG proceeds to filter its user links, selecting and employing those that are most perpendicular to the trajectory. One or more paths can be established to

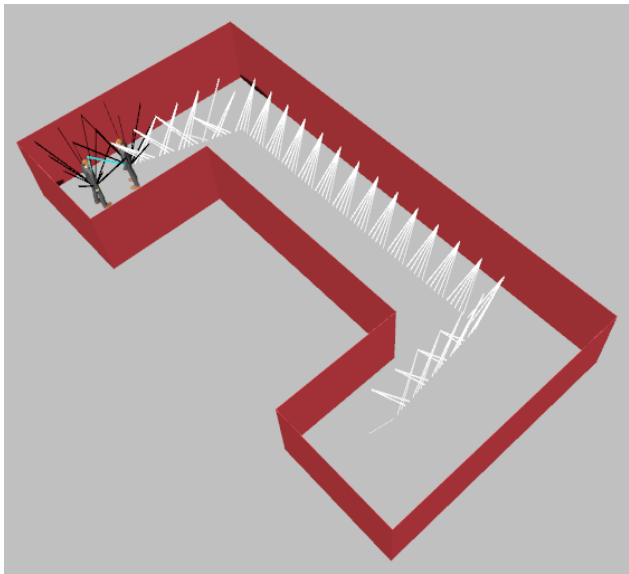


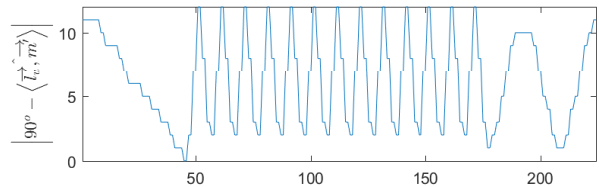
Fig. 9. Selected user links for Doppler effect mitigation across a trajectory.

connect the pair, using one or more of the user 0 links. We are interested in keeping the maximal deviation from perpendicularity bounded; the maximal angle formed by each user link and the trajectory must not exceed $90^\circ \pm 10^\circ$. If no user link fulfills this criterion, the link with the minimal deviation is selected.

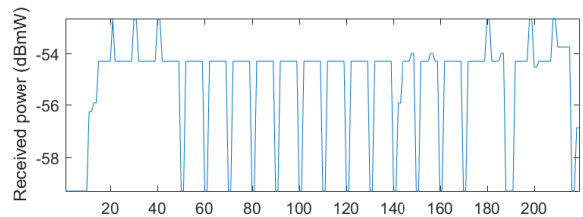
The user links selected across the trajectory are illustrated in Fig. 9 as white lines. As the user moves, he is served by the tile nearest to him. This tile remains active for a few steps and is then succeeded by another one. When a user is exactly below each active tile, its deviation from perpendicularity becomes minimal. The deviation then increases until the user is positioned exactly below the next active tile. This effect is shown in Fig. 10a, which also showcases the effect of tile placement across the trajectory. For the first 50 steps, the user follows a skewed direction with regard to the regular grid of the ceiling tiles (cf. the inset of Table V). As such, the tile selection and deviation does not exhibit a well-defined pattern. For steps 50 – 175, the trajectory is aligned with tile centers at the ceiling, exhibiting the described periodicity in the perpendicularity deviation. The pattern changes again for the last, skewed part of the trajectory.

Figure 10b shows the received power across the trajectory. It is worth noting that the received power drops when the deviation from perpendicularity spikes. Due to the user link selection process described above, only one connecting path may be active in these cases. This naturally limits the received power as well. Intermediate points in the trajectory allow for 2 or 3 concurrent paths, increasing the total carried power.

Finally, notice that the upwards directivity of the antennas means that there is no LOS component across the trajectory. Moreover, the use of collimation tile functions means that power losses are mainly encountered over the user links (cf. Fig. 4). However, the user link effects are static in this scenario, due to the upwards directivity of the antennas. Thus,



(a) Trajectory-to-propagation path perpendicularity.



(b) Received power.

Fig. 10. Trajectory-to-propagation path perpendicularity and receiver power across the user trajectory. (The x-axis represents steps of ~ 12.5 cm across the trajectory).

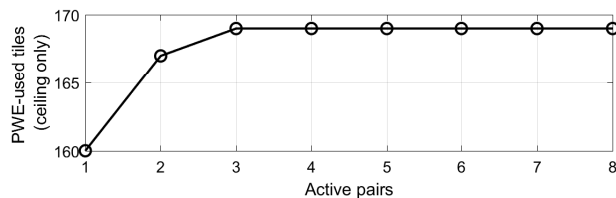


Fig. 11. Tiles activated (out of 169 total) as the number of user pairs increases, corresponding to the case of Fig. 12c.

the received power is mainly affected by the paths deployed between users 0 and 1.

C. User Capacity and Stress test

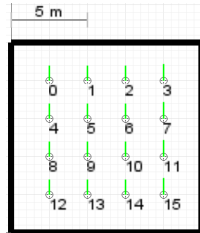
The final test studies the capacity of a PWE, subject to a configuration algorithm such as KPCONFIG. In other words, we seek to understand the conditions under which the PWE performance gains diminish to non-PWE levels.

The scenario setup is given in Table VI. It comprises 8 communicating pairs and three system stress levels. In the first level all transmitters have antennas with $\alpha = 50^\circ$, while the HyperSurface coating is full over walls, floor and ceiling (494 tiles total). The second stress level is the same but with $\alpha = 80^\circ$, naturally leading to more emitted rays to handle per transmitter. The last stress level is similar to the second, but only the ceiling is HyperSurface-coated (169 tiles total). Thus, the ray control points are fewer. Notice that partial coatings can be accounted for in KPCONFIG by passing a graph input \mathcal{G} that already contains tiles with $f_h \neq \emptyset$. In other words, areas without tile coating are marked as having virtual tiles, pre-configured with functions describing natural propagation. Finally, all user antennas are pointing upwards, yielding only NLOS components for all pairs.

Figure 12 presents the received power and interference among users per stress level, as well as the number of rays

TABLE VI
SCENARIO SETUP FOR THE PWE STRESS TEST.

USER: POSITION, α, ϕ	
0:	[2.5,10.0,1.0],{50°,80°},90.0°
1:	[5.0,10.0,1.0],{50°,80°},90.0°
2:	[7.5,10.0,1.0],{50°,80°},90.0°
3:	[10.0,10.0,1.0],{50°,80°},90.0°
4:	[2.5,7.5,1.0],{50°,80°},90.0°
5:	[5.0,7.5,1.0],{50°,80°},90.0°
6:	[7.5,7.5,1.0],{50°,80°},90.0°
7:	[10.0,7.5,1.0],{50°,80°},90.0°
8:	[2.5,5.0,1.0],180.0°,90.0°
9:	[5.0,5.0,1.0],180.0°,90.0°
10:	[7.5,5.0,1.0],180.0°,90.0°
11:	[10.0,5.0,1.0],180.0°,90.0°
12:	[2.5,2.5,1.0],180.0°,90.0°
13:	[5.0,2.5,1.0],180.0°,90.0°
14:	[7.5,2.5,1.0],180.0°,90.0°
15:	[10.0,2.5,1.0],180.0°,90.0°
PAIR: OBJECTIVE	
$(i) \rightarrow (15 - i), i = 0 \dots 7 :$	
	MAXPOWER,EAVMit[[ALL]]



impinging per tile in boxplot form. (All tiles are considered, virtual or real, active or inactive). In the first stress level, the PWE is configured by the KPCONFIG almost ideally (cf. Fig. 12a). The intended pairs are connected and well-separated. Minor interference is noticed explained as follows: with $\alpha = 50^\circ$, the affected tiles per transmitter marginally overlap. KPCONFIG configures roughly 20% of the available tiles ($101/494$). The tile re-use remains at very low levels, with 1 ray per tile being the most common case, as intended. The non-PWE does not exhibit a well-defined pattern and yields approximately 30 dBmW of extra loss per pair, and complete disconnection for 3 pairs.

The second stress level follows the same pattern but with decreased performance in both PWE and non-PWE (Fig. 12b). The PWE case continues to show good pair connectivity (notice the diagonal of intended pairs), but interference has increased as expected. KPCONFIG configures almost 50% of the available tiles ($256/494$). The same effect is evident in the non-PWE case, validating the presence of increased system stress. The tile re-use is kept low in the PWE case.

The final stress case shows a collapse in the PWE performance, making it almost indistinguishable from the non-PWE case (Fig. 12c). KPCONFIG uses all available tiles ($169/169$). The high stress level is also evident from the tile reuse, which is almost identical for both PWE and non-PWE. In Figure 11 we execute the same measurements as in Fig. 12, but by activating the transmitters in a serial fashion. Evidently, after a single transmitter is activated, almost all of the PWE tiles are used. This is natural, given that an antenna lobe of $\alpha = 80^\circ$ pointing upwards affects almost all of the ceiling tiles. Subsequent transmitters find no available free tiles to handle them, leading to uncontrolled propagation. Thus, at this point the user capacity of the PWE, *subject to KPCONFIG as the configuration scheme*, has been exceeded.

VI. DISCUSSION AND FUTURE WORK

The proposed KPCONFIG algorithm constitutes a first of its kind approach for configuring PWEs, with multi-user support and versatility in expressing resource sharing policies and user communication objectives. Moreover, it allows for expressing aspects of Physics in the form of graph models and algorithms. Thus, it can provide a new field of application for computer science concepts. For instance, subsequent studies can study the relation between the form of PWE graphs and the user capacity, as well as propose policies and alternative schemes that behave better under stress.

While KPCONFIG was employed in the preceding Sections for PWEs that were either fully or partially coated with HyperSurface tiles. The partially coating was arbitrarily set, to evaluate PWEs in a challenged setup. However, partial coatings have the benefits of reduced cost and easier deployment. In this aspect, deducing the partial PWE coatings that yield maximal performance gains constitute a promising approach for future research.

Handling transience, such as user mobility, was accomplished by executing KPCONFIG each time a change is detected in the environment. Nonetheless, future extensions can take into account the current PWE configuration, in order to minimize the changes in tile configurations. For instance, minor changes in the location of a user may be accommodated by modifying the last link of a path, rather than computing it from scratch.

Additionally, as noted in preceding Sections, a PWE can only control the NLOS component of communication, thus yielding a partial control over propagation. Nonetheless, the control can be made full, assuming joint collaboration with beamforming capabilities at the user devices. As shown in Section V, a device may seek to always emit towards a HyperSurface-coated area first, thus eliminating the LOS component and allowing for fully deterministic propagation in total. Notice that NLOS in PWEs can yield exceptional performance. Floorplan ceilings constitute good candidate-surfaces for applying HyperSurface coatings given that: i) they are largely unused, ii) they rarely contain obstacles, iii) they provide easy access to power supply via the existing power lines for lights, and iv) they pose strong security and interference mitigation benefits [6]. Thus, when present within a PWE, device gyroscopes can detect the upwards directions and beamform for emissions accordingly.

Finally, it is noted that KPCONFIG operates on the premise of limiting tile re-use among users and function combinations in general. However, future HyperSurface hardware technologies may provide perfect performance for combined functions. In such scenarios, the core PWE objective can be to minimize the number of activated tiles, thereby favoring tile re-use.

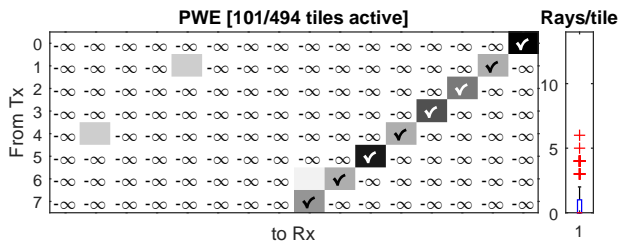
VII. CONCLUSION

Programmable wireless environments enable the customization of wireless propagation within them. The present work presented a novel scheme—the KPCONFIG—to configure such environments for serving multiple users and multiple objectives. Exemplary objectives include security against eavesdropping, mitigating Doppler effects, power transfer and

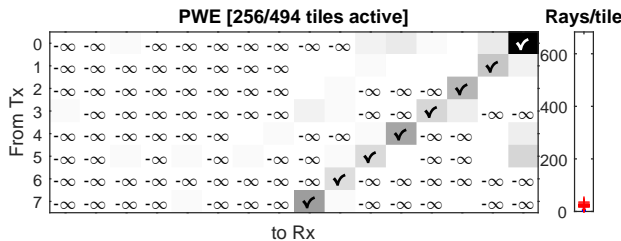
signal-to-interference maximization. KPCONFIG employs a novel, graph-based model of programmable environments, which transforms performance objectives to path search problems, while taking into account core Physical restrictions. KPCONFIG was extensively evaluated in a novel tool for simulating programmable wireless environments, yielding significant performance gains over regular propagation and reaching insights on the user capacity of PWEs.

REFERENCES

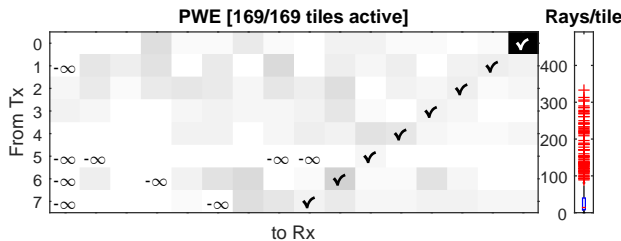
- [1] C. Liaskos *et al.*, "Using any surface to realize a new paradigm for wireless communications," *Communications of the ACM*, vol. 61, no. 11, pp. 30–33, 2018.
- [2] A. Li *et al.*, "Metasurfaces and their applications," *Nanophotonics*, vol. 7, no. 6, pp. 989–1011, 2018.
- [3] H. Yang *et al.*, "A programmable metasurface with dynamic polarization, scattering and focusing control," *Scientific reports*, vol. 6, 2016.
- [4] X. Tan *et al.*, "Enabling indoor mobile millimeter-wave networks based on smart reflect-arrays," in *Proceedings of IEEE Infocom'18*.
- [5] A. Welkie *et al.*, "Programmable radio environments for smart spaces," in *Proceedings of ACM HotNets'17*, pp. 36–42.
- [6] C. Liaskos *et al.*, "A novel communication paradigm for high capacity and security via programmable indoor wireless environments in next generation wireless systems," *Ad Hoc Networks*, vol. 87, pp. 1–16, 2019.
- [7] G. Coviello *et al.*, "Effects on phased arrays radiation pattern due to phase error distribution in the phase shifter operation," *MATEC Web of Conferences*, vol. 76, p. 03002, 2016.
- [8] L. Subrt and P. Pechac, "Intelligent walls as autonomous parts of smart indoor environments," *IET Communications*, vol. 6, no. 8, 2012.
- [9] X. Tan *et al.*, "Increasing indoor spectrum sharing capacity using smart reflect-array," in *Proceedings of IEEE ICC'16*.
- [10] Y.-H. Pao and V. Varatharajulu, "Huygens' principle, radiation conditions, and integral formulas for the scattering of elastic waves," *The Journal of the Acoustical Society of America*, vol. 59, no. 6, 1976.
- [11] C. Liaskos, A. Tsioliariidou *et al.*, "Initial uml definition of the hypersurface programming interface and virtual functions," *European Commission Project VISORSURF: Accepted Public Deliverable D2.1, 31-Dec-2017*, [Online:] <http://www.visorsurf.eu/m/VISORSURF-D2.1.pdf>.
- [12] C. Liaskos, A. Ptilakis *et al.*, "Initial uml definition of the hypersurface compiler middle-ware," *European Commission Project VISORSURF: Accepted Public Deliverable D2.2, 31-Dec-2017*, [Online:] <http://www.visorsurf.eu/m/VISORSURF-D2.2.pdf>.
- [13] C. Liaskos *et al.*, "A new wireless communication paradigm through software-controlled metasurfaces," *IEEE Communications Magazine*, vol. 9, pp. 162–169, 2018.
- [14] S. Abadal *et al.*, "Computing and communications for the software-defined metamaterial paradigm," *IEEEAccess*, vol. 5, pp. 6225–35, 2017.
- [15] C. Liaskos *et al.*, "Realizing wireless communication through software-defined hypersurface environments," in *Proc. of IEEE WoWMoM'18*.
- [16] I. F. Akyildiz, C. Han, and S. Nie, "Combating the distance problem in the millimeter wave and terahertz frequency bands," *IEEE Communications Magazine*, vol. 56, no. 6, pp. 102–108, 2018.
- [17] L. Zhang *et al.*, "Space-time-coding digital metasurfaces," *Nature Communications*, vol. 9, no. 1, 2018.
- [18] H. Wakatsuchi *et al.*, "Waveform-dependent absorbing metasurfaces," *Physical Review Letters*, vol. 111, no. 24, 2013.
- [19] M. J. Lockyear *et al.*, "Microwave surface-plasmon-like modes on thin metamaterials," *Physical Review Letters*, vol. 102, no. 7, 2009.
- [20] H.-T. Chen *et al.*, "A review of metasurfaces," *Reports on progress in physics*, vol. 79, no. 7, 2016.
- [21] A. Tsioliariidou *et al.*, "A novel protocol for network-controlled metasurfaces," in *Proceedings of the ACM NANOCOM'17*.
- [22] Pulse Power and Measurement Ltd., "Electric field (d-dot) sensors." [Online]. Available: <https://ppmtest.com/product-category/e-field-sensors/>
- [23] A. Ptilakis *et al.*, "Software-defined metasurface paradigm: Concept, challenges, prospects," in *Proceedings of METAMATERIALS'18*.
- [24] A. C. Tasolamprou *et al.*, "Intercell wireless communication in software-defined metasurfaces," in *Proc. of IEEE ISCAS'18*.
- [25] A. V. Volynskiy *et al.*, "Optical vortex generation and jones vector formalism," *Optics & Spectroscopy*, vol. 93, no. 2, pp. 267–272, 2002.
- [26] C. L. Holloway *et al.*, "An overview of the theory and applications of metasurfaces," *IEEE Ant. and Propag. Mag.*, vol. 54, pp. 10–35, 2012.
- [27] K. Guan *et al.*, "On millimeter wave and thz mobile radio channel for smart rail mobility," *IEEE Transactions on Vehicular Technology*, vol. 66, no. 7, pp. 5658–5674, 2017.
- [28] A. W. Brander and M. C. Sinclair, "A comparative study of k-shortest path algorithms," in *Performance Engineering of Computer and Telecommunications Systems*. Springer, 1996, pp. 370–379.
- [29] XJ Technologies, *The AnyLogic Simulator*, 2018. [Online]. Available: <http://www.anylogic.com/>
- [30] Q. Wu and R. Zhang, "Intelligent reflecting surface enhanced wireless network," *arXiv:1809.01423*, 2018.



(a) Full tile coverage, $\alpha = 50^\circ$ for each transmitter.



(b) Full tile coverage, $\alpha = 80^\circ$ for each transmitter.



(c) Partial tile coverage (ceiling only), $\alpha = 80^\circ$ for each transmitter.

Fig. 12. Power reception and tile reuse for various test of progressively increasing stress. ✓ denotes intended pair connectivity. The colormap is common across all subplots: $[-106.94 \text{ } \blacksquare \text{ } -59.23] \text{ dBmW}$.